Supporting information

Online measurement of glucose consumption from HepG2 cells using an integrated bioreactor and enzymatic assay

Anna G. Adams,[§] Radha Krishna Murthy Bulusu,[†] Nikita Mukhitov, [§,‡] Jose L. Mendoza-Cortes, [†,‖] and Michael G. Roper[§,*]

[§]Department of Chemistry and Biochemistry, Florida State University, 95 Chieftain Way, Tallahassee, FL 32306

[†]Department of Chemical & Biomedical Engineering, FAMU-FSU College of Engineering, 2525 Pottsdamer Street, Tallahassee, FL 32310

[‡]Department of Biological Engineering, Massachusetts Institute of Technology, Cambridge, Massachusetts, 02139

[‖]Department of Physics, Scientific Computing, Materials Science and Engineering Program, High Performance Materials Institute, & Condensed Matter Theory, National High Magnetic Field Laboratory (NHMFL), Florida State University, 1800 E Paul Dirac Dr, Tallahassee, FL 32310

Correspondence and requests for materials should be addressed to:

*M.G.R.: Phone: 850-644-1846, Fax: 850-644-8281. Email: roper@chem.fsu.edu

Included in the Supporting information is a detailed description of droplet analysis. Also, SEM images, measurements, and finite element analysis of pressure, velocity, and shear stress in the microfluidic bioreactor. Additionally, metabolic characterization of the HepG2 cells and calibration of the glucose measurement in the presence of insulin are included. Finally, all data traces from HepG2 experiments are provided.

Droplet analysis.

Since the individual droplets were not resolved using the parameters for the glucose measurements, a faster exposure time of 1.5 ms was used with bright field imaging. Three sequential images of droplet formation (an example of one image is shown in **Figure S-5**) were obtained using the same flow rate parameters of the oil and aqueous solutions as stated in the text. The average (± SD) number of droplets in each image was 17 ± 1. From these images, we measured the average (± SD) droplet width to be 289 ± 6 μm (n = 104 droplets).

The total volumetric flow rate of the aqueous and oil solutions was 25 μL min^{-1}, and given the channel dimensions of the droplet device, the linear velocity of the solution was 5.6 mm s^{-1}. In a 42 ms exposure, the distance a single droplet traveled was ~240 μm, or approximately the diameter of a single droplet. We therefore estimate that the number of droplets measured during the 42 ms exposure was 18.

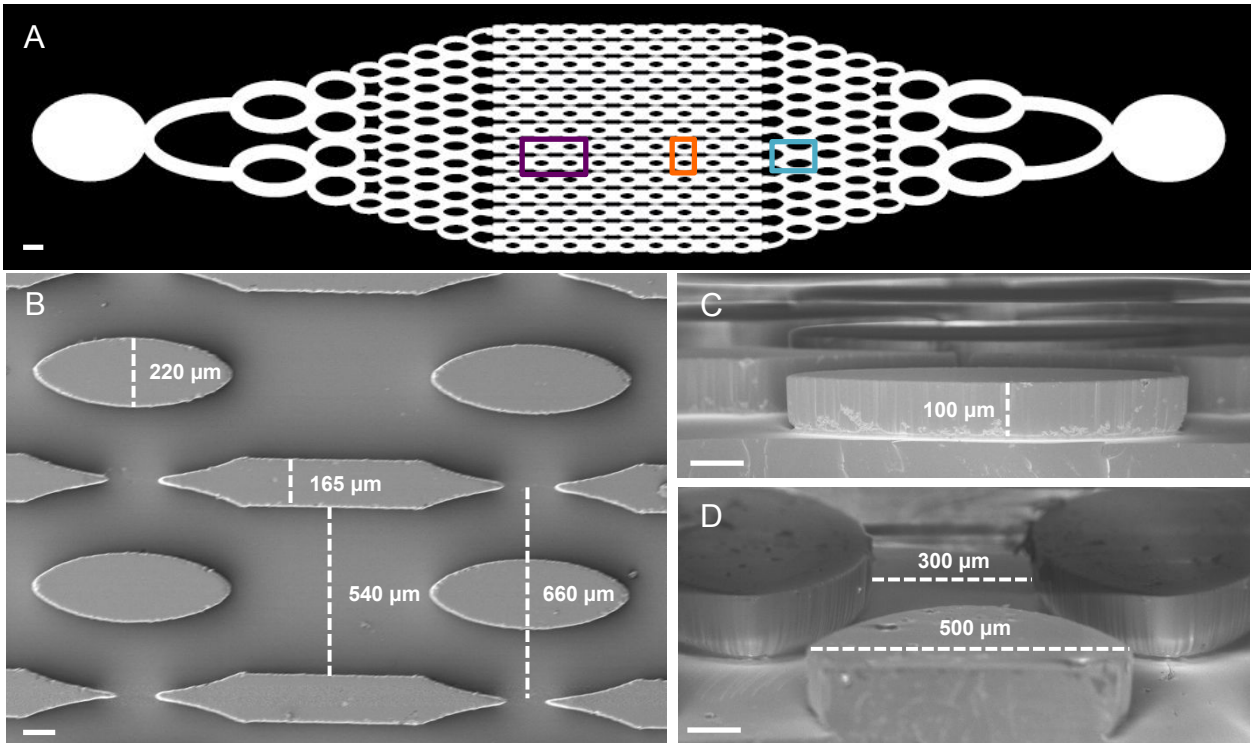

Figure S-1. **Details of the bioreactor. A.** The image of the photomask used to create the bottom layer of the bioreactor is shown. On the left side is the inlet which branches to the cell culture region. The channels after the cell culture region then converge back to a single outlet on the right. The scale bar on the bottom left of the image is 1 mm. **B**. A micrograph (60X magnification) of the area highlighted in purple in **A**. The channels (dark shaded regions) and structures (light shaded regions) in the cell chamber are shown with the dimensions of the features. **C**. A micrograph (140X magnification) from the horizontal direction of the region highlighted in orange in **A**. Hepatocytes attach and grow on the sides or on top of this post, or in the channel around it. **D**. A 140X magnified image of a rotated horizontal slice from the area highlighted in cyan in **A** showing the exit channel where media flows out of the bioreactor. In **B-D**, scale bars in the bottom left correspond to 100 µm.

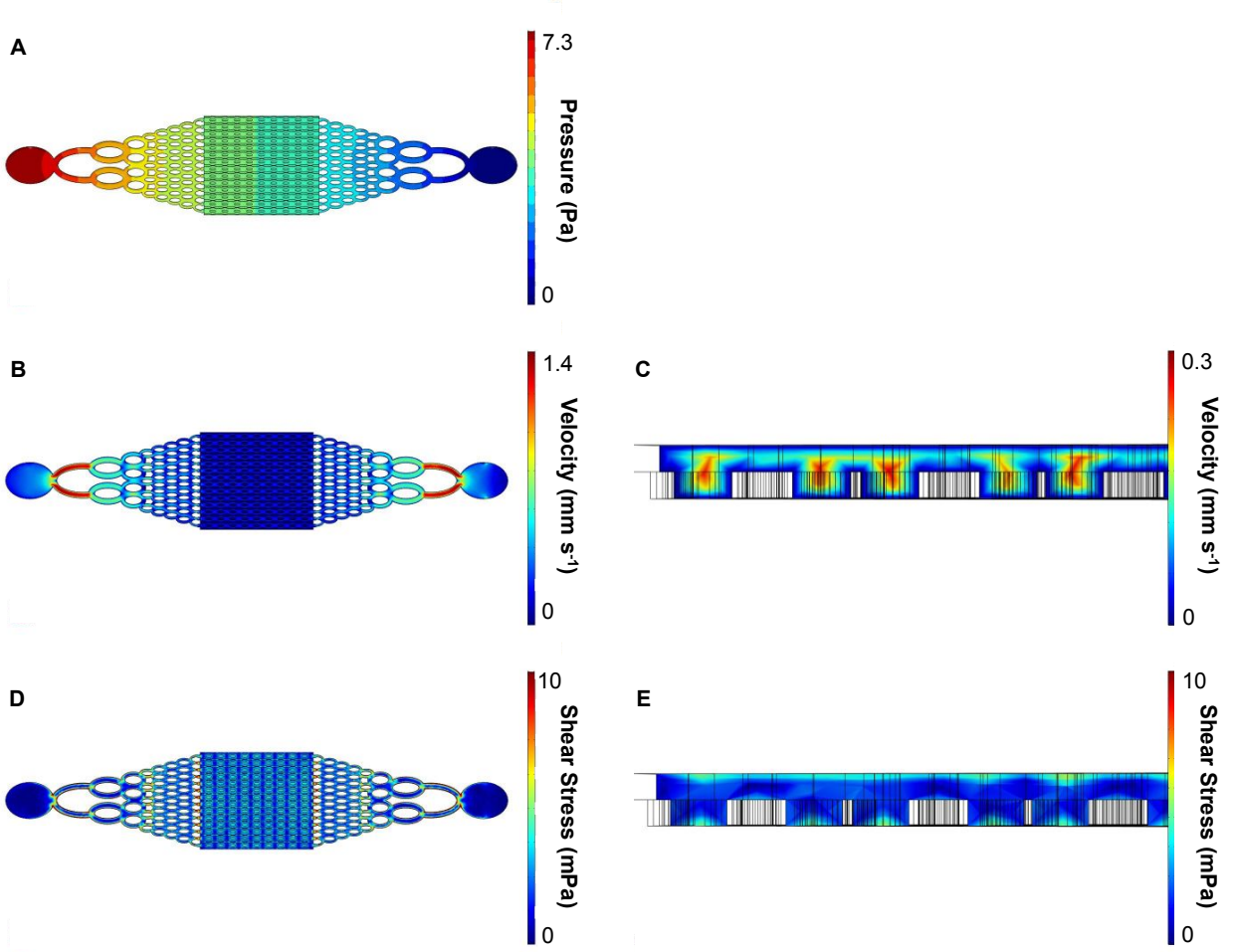

Figure S-2. Finite element analysis of pressure, velocity, and shear stress in bioreactor. **A.** A top-view of the bioreactor showing the linear pressure drop across the device. **B.** The resulting 2D velocity simulation is shown. **C.** The velocity simulation across a cut-slice through the center of the device showing high linear velocity in the regions between the posts. **D.** The shear stress is shown across the entire device with maximum values less than 10 mPa. **E.** The shear stress through the center of the device is shown.

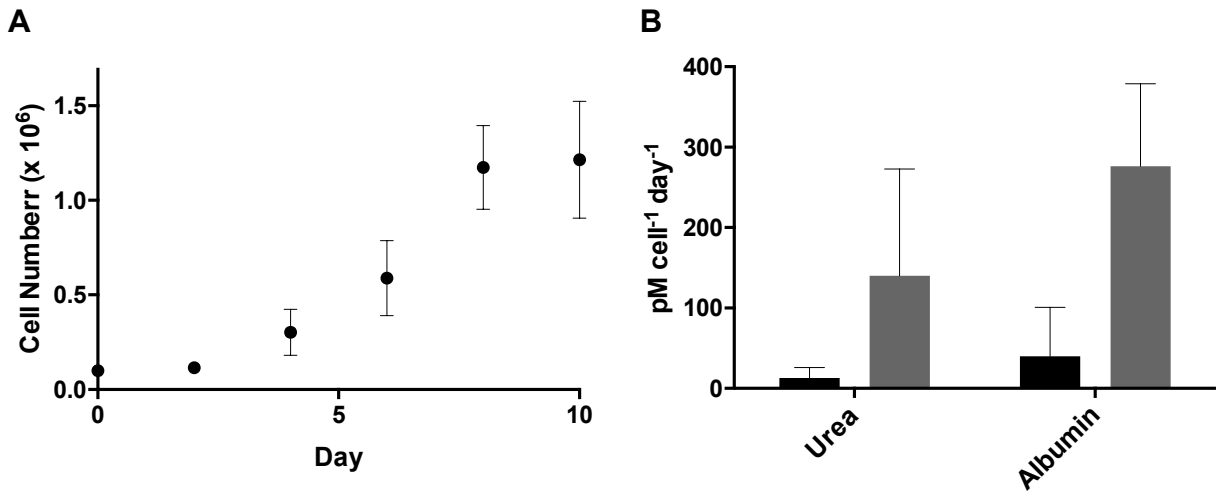

Figure S-3. 10-day growth curve and metabolic activity of HepG2. A. 10-day growth curve of HepG2 is shown. Data points are the average number of HepG2 cells from three bioreactors, counted every other day. **B.** The average urea and albumin concentration normalized per HepG2 cell and day, over a 10-day period is shown for 2D culture (black bars) and 3D culture (grey bars). Error bars correspond to ± 1 SD.

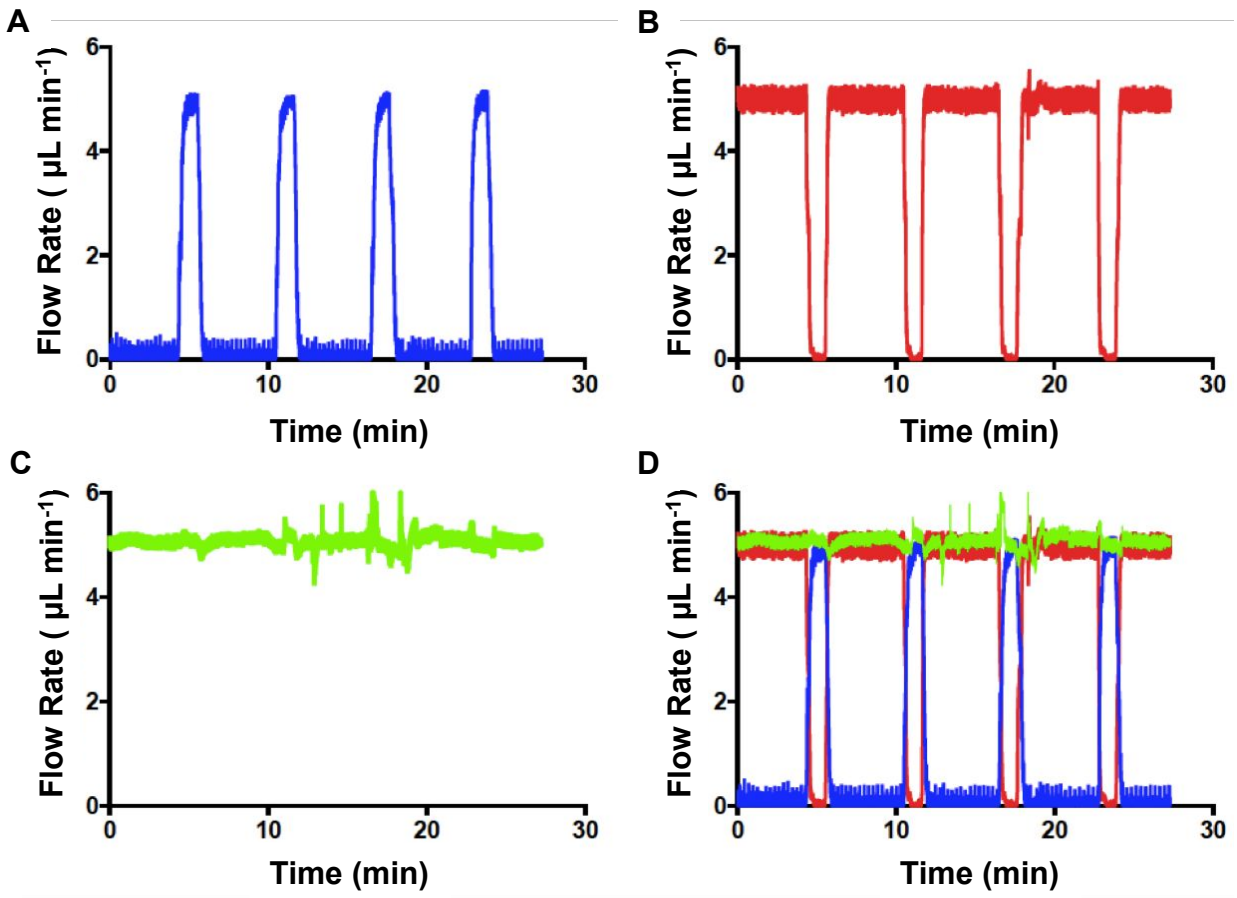

Figure S-4. **Flow profiles of each solution in Figure 1A. A.** The flow rate as a function of time for the reservoir that contained 10 mM glucose and 200 nM insulin. For the majority of time, the flow rate was 0 µL min^{-1}, but when insulin was required, the flow rate increased to 5 µL min^{-1}. **B.** The flow rate from the reservoir containing only 10 mM glucose is shown. The opposite profile to that in **A** was delivered where the majority of time the flow was 5 µL min^{-1} and during the times of insulin delivery, the flow rate dropped to 0 µL min^{-1}. **C.** The flow rate from the reservoir that housed the assay reagents is shown. This flow remained constant during the course of experimentation at 5 µL min^{-1}. Slight fluctuations in the flow rate were due to the low volume in the reservoir (< 2 mL) that made it more sensitive to the feedback from the flow sensor and pressure regulator. **D.** The flow rates of all sensors are overlaid. The flows shown in A and B are timed such that the total flow rate to the bioreactor remains constant at 5 µL min^{-1} despite the individual changes to the reservoirs. The assay reagents maintained a constant flow rate to ensure a 1:1 ratio of assay reagent to sample, producing a total overall flow rate of 10 µL min^{-1} to the droplet device.

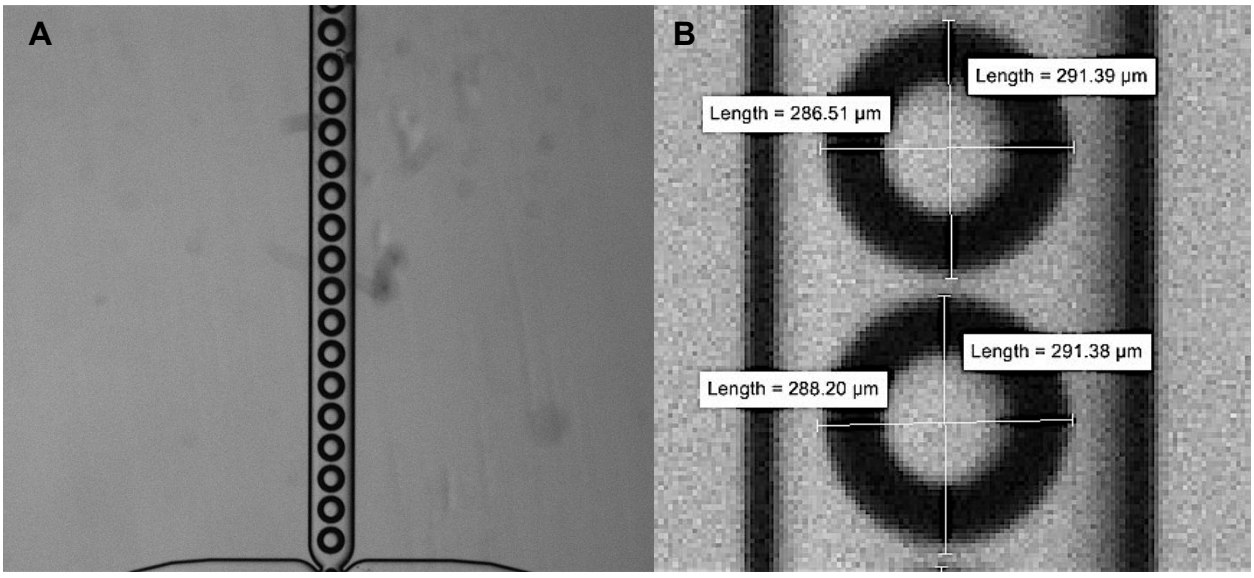

Figure S-5. Droplet analysis. In both images, the channel width is 390 µm. **A.** Brightfield image of droplets in the channel at 1.5 ms exposure. There are 17 droplets in the 5.68 mm long channel. **B**. Shown is a zoomed-in view of two droplets and their measured length. Droplets in three sequential images were measured and found to be 288 ± 7 µm (n = 51 droplets).

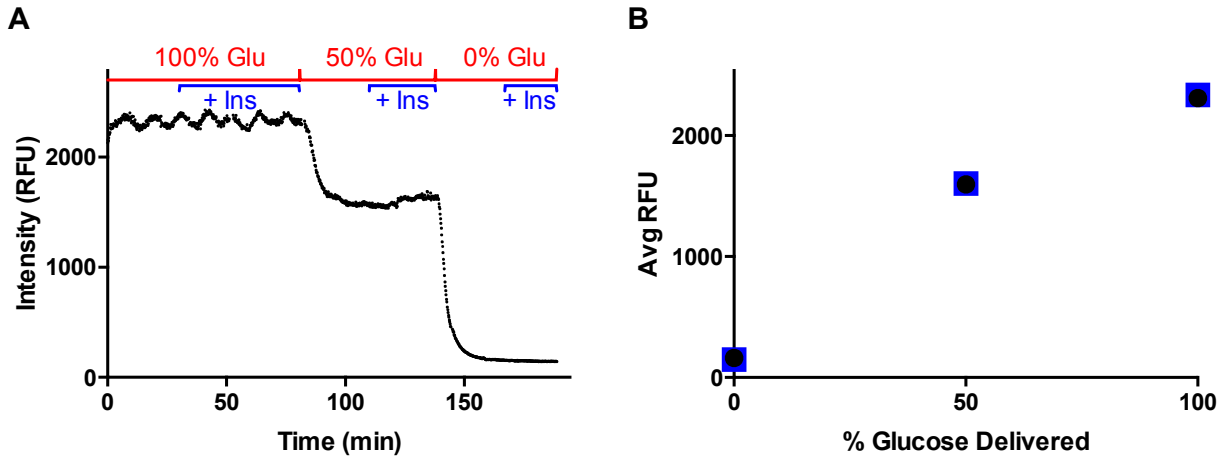

Figure S-6. The effect of insulin on glucose assay. A. The measured glucose output was recorded during delivery of 100%, 50%, and 0% of 12 mM glucose with and without 200 nM insulin. **B.** The average relative fluorescence units as a function of glucose delivered with 200 nM insulin (blue squares, $y = 22x + 265$, $r^2 = 0.97$) and without insulin (black circles, $y = 22x + 277$, $r^2 = 0.97$). Error bars correspond to ± 1 SD of the measurements.

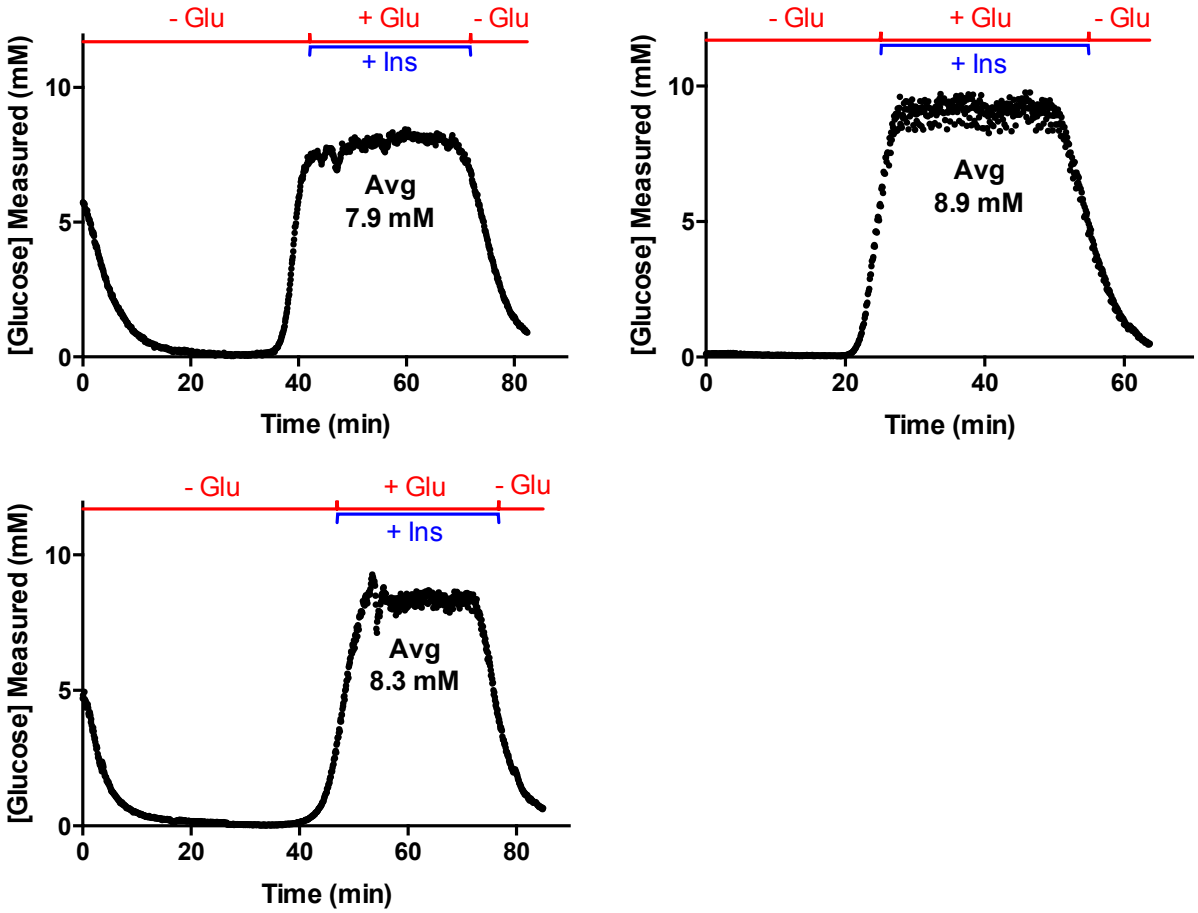

Figure S-7. Delivery of insulin to hepatocytes. Glucose output traces of three experiments consisting of perfusion with 0 mM glucose to initiate glycogen depletion, followed by perfusion with 200 nM insulin in 10 mM glucose, ending with perfusion with 0 mM glucose. The average glucose output during delivery of glucose and insulin is shown in the plots.

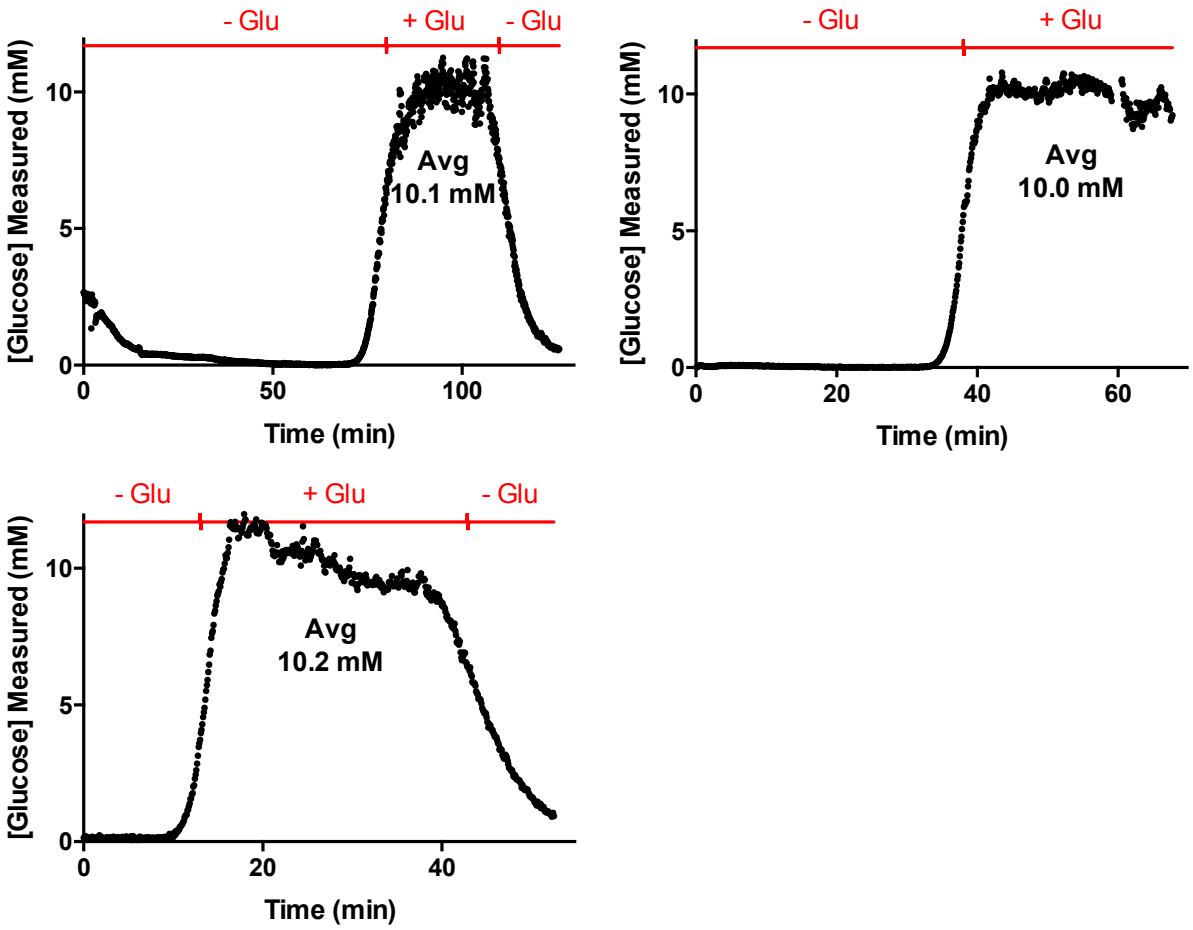

Figure S-8. Delivery of glucose to hepatocytes. Glucose output traces of three experiments consisting of perfusion with 0 mM glucose to initiate glycogen depletion, followed by perfusion with 10 mM glucose without insulin. The average glucose concentration during perfusion with 10 mM glucose is shown in each trace.

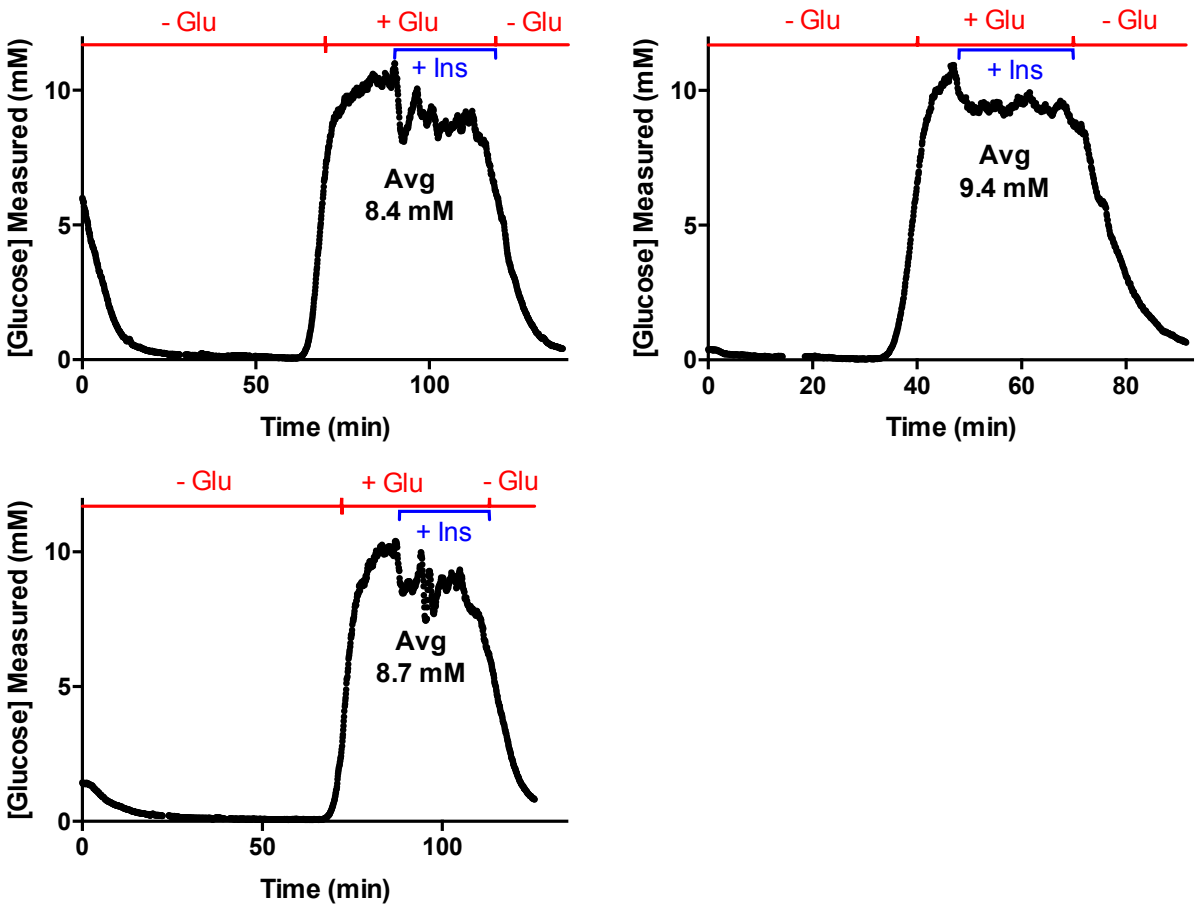

Figure S-9. Dynamic insulin perfusion experiments. Glucose output traces of three experiments consisting of perfusion with 0 mM glucose to initiate glycogen depletion, followed by perfusion with 10 mM glucose, followed by perfusion with 200 nM insulin in 10 mM glucose, and ending with perfusion with 0 mM glucose. The average glucose level during perfusion of glucose and insulin is provided in each plot.

Table S-1.

Figure	Experiment	High Glucose Perfusion (min)	Avg Measured [Glucose] (mM)	Standard Deviation (mM)	Number of Data Points
3A		**+ Ins**			
	1	30	7.9	0.3	359
	2	30	7.9	0.3	358
	3	30	8.3	0.4	358
	4	30	8.9	0.6	358
3B		**- Ins**			
	1	30	9.9	0.3	360
	2	30	10.0	0.4	361
	3	30	10.2	0.8	358
	4	30	10.1	0.5	358
4A		**+ Ins**			
	1	21	8.1	0.6	251
	2	22	9.4	0.2	263
	3	25	8.4	0.8	300
	4	29	8.7	0.5	349
		- Ins			
	1	14	10.1	0.3	168
	2	8	10.1	0.5	95
	3	16	10.0	0.2	192
	4	20	10.2	0.3	239
4B		**+ Ins**			
	1	21	9.4	0.9	239
	2	25	8.4	0.9	299
		- Ins			
	1	15	10.2	0.3	179
	2	13	9.8	0.6	150